Science of the Total Environment 813 (2022) 152651

Contents lists available at ScienceDirect

Science of the Total Environment

journal homepage: www.elsevier.com/locate/scitotenv

Research Paper

Spatiotemporal variations of surface ozone and its influencing factors across Tibet: A Geodetector-based study

Yan Chen [a,b], Yunqiao Zhou [a,*], NixiaCiren [c], Huifang Zhang [c], Caihong Wang [c], GesangDeji [c], Xiaoping Wang [a,b,*]

[a] State Key Laboratory of Tibetan Plateau Earth System, Resources and Environment (TPESRE), Institute of Tibetan Plateau Research, Chinese Academy of Sciences, Beijing 100101, China
[b] University of Chinese Academy of Sciences, Beijing 100049, China
[c] Tibetan Ecology and Environment Monitoring Center, Lhasa 850000, China

HIGHLIGHTS

- The annual mean concentrations of surface ozone showed an increasing trend.
- Surface ozone were higher in the northwest, lower in the southeast and northeast.
- Surface ozone distribution was mainly controlled by natural factors.
- RH∩PM_{10} (q = 0.77) exhibited the strongest impact on surface ozone distribution.

GRAPHICAL ABSTRACT

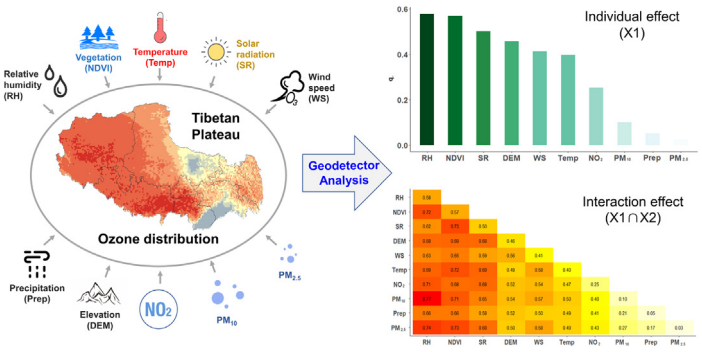

ARTICLE INFO

Article history:
Received 31 August 2021
Received in revised form 22 November 2021
Accepted 20 December 2021
Available online 23 December 2021

Editor: Jianmin Chen

Keywords:
Surface ozone
Spatiotemporal variation
Geodetector
Influencing factor
Tibet

ABSTRACT

Reasons regarding surface ozone formation and distribution in remote regions is limited. Tibet is an important remote area on Earth, with various climates and extremely high elevation (average ~ 4000 m), which makes it a good place to study the spatiotemporal distribution of surface ozone and explore the causes. Based on ground monitoring data from 18 stations on Tibet between 2015 and 2019, the annual, seasonal, monthly, and diurnal variations of surface ozone were analyzed. The annual mean values (60.7–72.5 μg/m^3) presented an increasing trend during the past five years, with seasonal concentrations of surface ozone higher in spring than in winter. Spatially, both the ground observations and high-resolution remote sensing data indicated that the surface ozone was relatively high in the southwest regions of Tibet, and low in the southeast and northeast areas. Geodetector analysis found that relative humidity (RH), normalized difference vegetation index (NDVI), and solar radiation (SR) were the top three individual factors affecting surface ozone distribution, while NO_2, PM_{10}, and $PM_{2.5}$ showed less influence. All influencing factors showed an improvement through the two-factor interaction. The associations of RH∩PM_{10} (q = 0.77), RH∩NDVI (q = 0.72), and NDVI∩SR (q = 0.73) exhibited a strong impact on surface ozone distribution, suggesting that places with sparse vegetation cover, dry climate and strong SR would usually cause high atmospheric ozone burden. This could also explain why concentrations of surface ozone continue to increase in some remote areas worldwide with ecological deterioration and desertification.

* Corresponding authors at: State Key Laboratory of Tibetan Plateau Earth System, Resources and Environment (TPESRE), Institute of Tibetan Plateau Research, Chinese Academy of Sciences, Beijing 100101, China.
E-mail addresses: zhouyunqiao@itpcas.ac.cn (Y. Zhou), wangxp@itpcas.ac.cn (X. Wang).

http://dx.doi.org/10.1016/j.scitotenv.2021.152651

1. Introduction

High levels of surface ozone not only damage crops and plants (Agathokleous et al., 2020; Avnery et al., 2011; Feng et al., 2015), but also increase the risk of the population's mortality (Chen et al., 2017; Liu et al., 2018; Turner et al., 2016). A continuous increase in the concentration of surface ozone has become an emerging atmospheric environmental problem and arouses global concern (Cooper et al., 2015). The surface ozone concentration has presented an increasing trend of ~0.2 μg/m^3 per year since 1990 (Pierre, 2021). For example, at a remote place (Mace Head) of Ireland, the mean increase rate of surface ozone reached 0.43 μg/m^3 per year from 1987 to 2017 (Derwent et al., 2018). Similar increases were also reported for remote high-elevation sites, including Mt. Happo in Japan (Sunwoo and Carmichael, 1994), Jungfraujoch in Switzerland (Tarasova et al., 2009), and White Mountains in the USA (Burley and Bytnerowicz, 2011).

Basically, elevated temperature and increased concentrations of atmospheric pollutants (nitrogen dioxide, volatile organic compounds, etc.) were the possible contributors (Stepanov et al., 2019) that lead to rising ozone levels. Relative humidity, solar radiation, wind speed, long-distance transport from urban areas and stratospheric intrusion also affected the ozone concentration (Saliba et al., 2008; Yeo and Kim, 2021; Yin et al., 2017; Zhang et al., 2015). Despite of these results, the reasons for the increase and distribution of surface ozone in remote regions still remain limited.

Tibet with an average altitude of above 4000 m, is one of the highest remote regions in the world (Yao et al., 2012). The surface ozone displays remarkable spatial and temporal differences across Tibet. In northern part, the annual average concentrations of surface ozone around Waliguan Mountain (~3800 m) have increased from 45 to 55 μg/m^3 during a recent 15-year period (1995–2010) (Xu et al., 2016). However, the annual average concentrations of surface ozone in Lhasa (central Tibet) are relatively stable (Yin et al., 2019). Similarly, the maximum ozone concentrations occurred in summer in Waliguan site (Xu et al., 2016; Shen et al., 2014), while they reached a peak in the spring in southern Tibet (Cristofanelli et al., 2010).

Since Tibet covers such a vast area, studies based on ground monitoring stations (Lin et al., 2015; Shen et al., 2014; Yin et al., 2017) are unlikely to capture and explain the overall characteristics of ozone variation across Tibet. It requires the complement of remote sensing technology, by which high-resolution data of ozone concentration, and environmental variables (meteorological condition, vegetation coverage, and pollutant level) can be provided. Moreover, ozone formation and distribution can not be affected by a single factor; the associated impacts of two/multi-factors should be of great concern.

The Geodetector is a good method of spatial statistics for measuring and attributing spatial stratified heterogeneity (Wang et al., 2010). A key principle of its theory is to detect the consistency between spatial distribution patterns of dependent and independent variables, which can quantitatively determine the explanatory power of individual factors and two-factor interactions (Wang and Xu, 2017; Wang et al., 2020b). Due to these advantages, the combination of remote sensing data and Geodetector analysis can provide new insights regarding which factors influence ozone formation and distribution in Tibet.

Therefore, the aims of this study were to: (1) obtain the temporal variations of surface ozone across Tibet based on ground monitoring data from 2015 to 2019; (2) reveal the spatial distribution pattern of surface ozone using both ground and remote sensing data; (3) use Geodetector analysis to quantify the influence strength of individual factors on the variation of surface ozone and evaluate the associated impacts of two different factors. This study will provide new understanding into the features of surface ozone occurrence in remote regions and support governments in mitigating ozone pollution in the future.

2. Data and methods

2.1. Data source

Surface ozone concentration from 2015 to 2019 were obtained from the real-time air quality monitoring data released by the China National Environmental Monitoring Center. After discarding invalid data, there were 18 effective monitoring sites in 2015 and 2018, 16 in 2016 and 2019, and 17 in 2017 (Fig. 1). These sites can be grouped into seven regions: Lhasa, Shigatse, Lhokha, Nying, Chamdo, Nagchu, and Ngari. As shown in Fig. 1, it is clear that most ground monitoring sites are located in central and southern Tibet, and only very limited sites are in the west (e.g., Ngari). Thus, in order to obtain an accurate spatial distribution pattern of surface ozone across Tibet, remote sensing data (i.e., ChinaHighO_3) were included and compared with the ground monitoring data (Wei et al., 2022).

The reason for choosing the remote sensing data of 2018 was that the ground monitoring sites (18) in that year were relatively abundant, allowing a better comparison to ground monitoring data. Additionally, concentrations of surface ozone in 2018 were relatively great (72.5 μg/m^3). Thus, the remote sensing data of 2018 was deployed to test whether the Tibetan environment [elevation (DEM) and normalized difference vegetation index (NDVI)], meteorological conditions [temperature (Temp), relative humidity (RH), precipitation (Prep), solar radiation (SR), and wind speed (WS)], and anthropogenic factors ($PM_{2.5}$, PM_{10}, and NO_2) influence the formation, temporal trend (increase or decrease), or spatial distribution of surface ozone. The reasons for choosing these factors were available in the Supporting Information (SI, Fig. S1). Remote sensing data of surface ozone (i.e., ChinaHighO_3) were downloaded from the CHAP dataset in a previous study (Wei et al., 2022). The detailed description and source of these data are available in Table S1.

2.2. Research methods

In terms of the climatic features of Tibet (Yin et al., 2017), this study regarded March to May as spring, June to August as summer, September to November as autumn, and December to February as winter. Annual, seasonal, monthly, and diurnal variations of surface ozone across Tibet were calculated by the continuous five-year moving average method. Moran's *I* index was used to evaluate the spatial autocorrelation of surface ozone concentration. The Geodetector method was applied to indicate the influence strength of individual factors and their association effects.

Geodetector is a spatial statistical method to analyze the spatial variability of pollutants and reveal their potential driving factors (Wang and Xu, 2017). It can evaluate the effect of an individual factor as well as the associated effect of two different factors. All the results are quantified by the q value, which is calculated as follows:

$$q = 1 - \frac{1}{N\sigma^2}\sum_{z=1}^{L} N_z \sigma_z^2 \quad (1)$$

where *z* is the hierarchy of variable Y or factor X; N means the number of units, and σ_z^2 represents the variance value of variable Y.

Details of Moran's *I* and Geodetector are given in the SI. Judgment criteria of different interaction modes of Geodetector are listed in Table S2 and the software is downloaded for free on the website of http://www.geodetector.cn/.

2.3. Data preparation of influencing factors

The Geodetector analysis can only deal with discrete variables, and spatial grids with the same resolution of all the influencing factors are needed to match the variable Y (surface ozone concentration) and variable X (influencing factors) to acquire the q value. Therefore, the value of all the influencing factors, including $PM_{2.5}$, PM_{10}, NO_2, Temp, RH, Prep, SR, WS, DEM, and NDVI, were divided into nine categories (discrete variables) by the natural breaks tool in ArcGIS (Fig. S2). After the preparation, the values

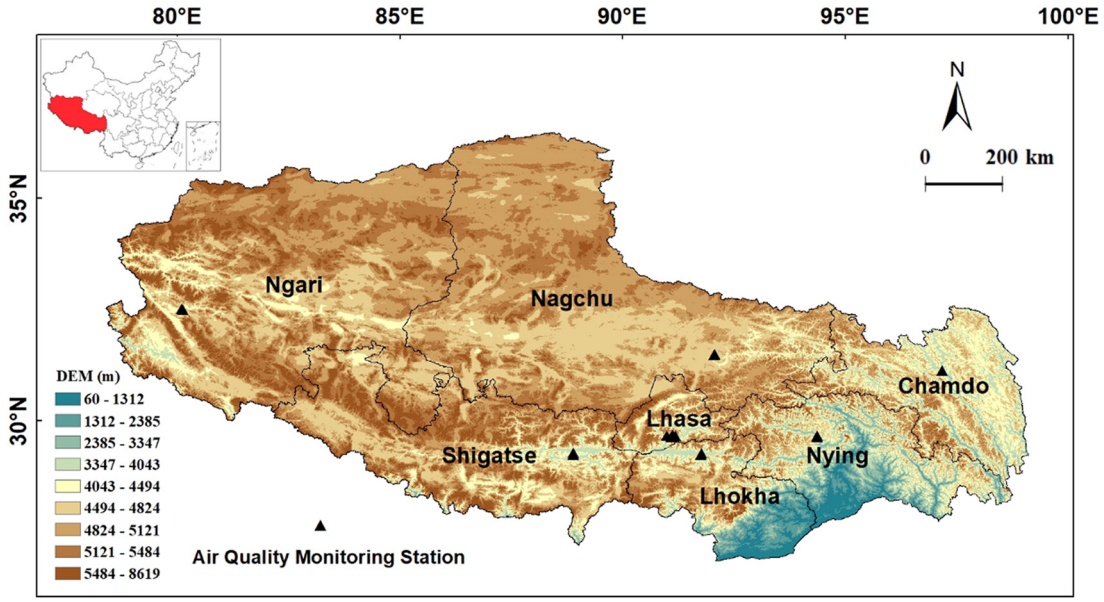

Fig. 1. Study area and the location of air quality monitoring stations in Tibet.

of influencing factors and the surface ozone concentrations were imported into the Geodetector software to conduct the analysis (Wang and Xu, 2017).

3. Results and discussion

3.1. Temporal evolution of surface ozone in Tibet from 2015 to 2019

3.1.1. Annual variation

During 2015–2019, annual average concentrations of surface ozone in Tibet varied within a narrow range, from 60.7 to 72.5 μg/m^3 (Fig. S3). Annual means of daily maximum 1-h average ozone concentration (MDA1) and daily maximum 8-h average ozone concentration (MDA8) were close and shared a similar variation tendency. The lowest annual average of MDA8 was 60.7 μg/m^3 observed in 2016, and the highest value was 72.5 μg/m^3 in 2018 (Fig. S3). The annual average of MDA8 in Tibet was higher than that in the Antarctic region (~55.6 μg/m^3) (Helmig et al., 2007) and Waliguan Mountain (~55 μg/m^3) (Xu et al., 2016), but lower than that in Beijing (100–120 μg/m^3) (Wang et al., 2020b) and Yangtze River Delta (>100 μg/m^3) (Xu et al., 2021). Overall, the surface ozone concentrations of Tibet were still at a low level but showed an upward trend.

The annual averages of MDA1 and MDA8 in the seven different regions of Tibet ranged from 28.9 to 90.7 μg/m^3 (Fig. S3 b,c), which were all below the strictest standard limit (100 μg/m^3) stated in the Chinese Ambient Air Quality Standard (GB3095–2012). Among these results, the highest average annual MDA1 (90.7 μg/m^3) occurred in Ngari in 2017, and the lowest value of 29.6 μg/m^3 was found in Nagchu in 2016. For annual average MDA8, the lowest value (28.9 μg/m^3) occurred in Nagchu in 2016, while the maximum value (89.1 μg/m^3) was in Ngari in 2017. Broadly, the interannual variations of MDA1 and MDA8 in most regions of Tibet were stable. However, an increase of surface ozone occurred in Lhokha after 2015, and in Nagchu and Ngari after 2016, and the difference between the maximum and minimum ozone concentrations was 1.5 and 2 times, respectively, in Nagchu and Ngari (Fig. S3).

3.1.2. Seasonal variation

MDA8 is adopted for the seasonal variation analysis since it represents more of the medium- and long-term impact of surface ozone (Maji and Namdeo, 2021; Shu et al., 2020; Zhan et al., 2018). In general, seasonal variations of surface ozone concentrations in Tibet were at their highest in spring (86.5 μg/m^3, Fig. 2a) and then decreased continuously to their lowest in autumn (56.3 μg/m^3, Fig. 2a). This pattern was different from the trend in some urban areas in plain regions, with the higher concentrations usually observed in summer (Wang et al., 2020b). Given the stratosphere-to-troposphere interaction over Tibet is more frequent in spring, it will cause the incursion of ozone from the stratosphere (Neu et al., 2014). Yin et al. (2017) found that this incursion's contribution to surface ozone variation can reach up to 20%. This is likely the reason for the spring maximum of surface ozone in most regions of Tibet.

Among the seven regions investigated in the present study (Fig. 1), Lhasa and Shigatse are the most populated areas, where may release more ozone precursors. Although the seasonal pattern of surface ozone in these two regions is similar to the average variation of the whole Tibet, the average seasonal MDA8 in Lhasa and Shigatse in spring exceeds the first-level limit (100 μg/m^3) (Fig. 2b). This suggests that the combined contributions of stratospheric incursion and local precursor oxidation likely resulted in the aggravation of surface ozone in spring across Tibet (Ran et al., 2014).

Contrary to most regions of Tibet, the lowest surface ozone concentration in Nying occurred in summer rather than autumn (Fig. 2b), similar to Shangri-La of Southern China (Ma et al., 2014) and the southern Himalayas of Nepal (Cristofanelli et al., 2010). The summer minimum may be the result of vegetation absorption, as the above-mentioned places (Nying, Shangri-La, southern Himalayas) have relatively dense forest coverage. Weak stratospheric input combined with vegetation absorption is thus the most likely reason to explain the summer minimum of surface ozone in southeast Tibet (Cristofanelli et al., 2010).

The peak time of surface ozone concentrations in Tibet is further depicted by the monthly variations shown in Fig. 2b. In terms of the different regions, the peak time of surface ozone concentrations in central and southern Tibet, including Lhasa, Shigatse, Lhokha, and Nying, occurred in April in the late spring (Fig. S4), with the values of 113.6, 111.2, 108.0, and 91.5 μg/m^3, respectively. Meanwhile, surface ozone concentrations in northern Tibet, such as Nagchu and Ngari, reached their highest values of 68.6 and 99.0 μg/m^3 in June in the early summer. Taking Qinghai Lake (higher latitude, peak time mid-June) into account (Shen et al., 2014), surface ozone concentrations vary with latitude, showing an earlier peak time in low latitudes and a later peak time in high latitude regions (Fig. S4). As the climate of Tibet (warm and wet in the south, dry and cold in the north), this difference in peak time (high concentrations occurred in the north a month later than in the south) indicated that meteorological conditions are likely the important influencing factors.

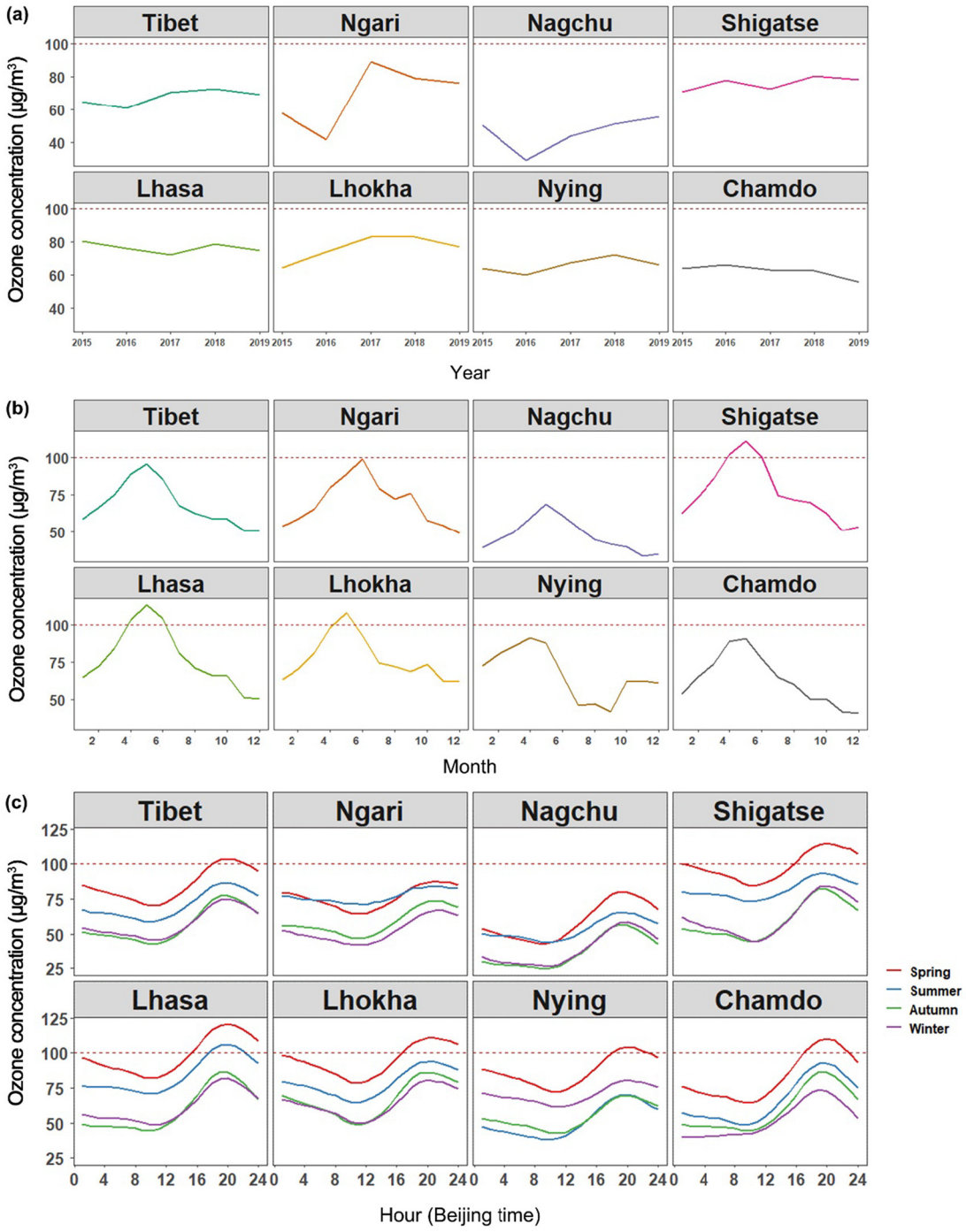

Fig. 2. Annual (a), monthly (b), and diurnal (c) variations of the average concentrations of surface ozone in different regions of Tibet.

3.1.3. Diurnal variation

Within a day, the surface ozone concentrations varied greatly, showing the lowest levels around 10:00 and the highest around 20:00 (UTC + 8, Beijing time), and the high/low ratio was about 1.5 to 2 (Fig. 2c). Additionally, the variation patterns were similar in all the regions and in all seasons, and were ranked as spring > summer > autumn > winter (Fig. 2c). Overall, concentrations of surface ozone increased in the morning, reached their peak in the afternoon, accompanied by sunrise and sunset, which was consistent with previous studies in Dangxiong (Lin et al., 2015), Namco (Yin et al., 2017), and other diurnal variation studies across Tibet (Chen et al., 2020). WS and SR usually increase in the afternoon, which further highlights the contribution of meteorological conditions to surface ozone levels. However, the results of this study were different from previous findings near northern Tibet (in Waliguan Mountain the diurnal ozone concentrations were almost stable), where weak valley wind was considered to be the main influencing factor (Xue et al., 2011).

3.2. Spatial distribution of surface ozone in Tibet in 2018

Based on the above analysis, we know that surface ozone concentrations vary greatly as Tibet is a vast area with a changeable climate. Before investigating the contributions of different influencing factors, the spatial distribution pattern of surface ozone needs to be depicted. In this study, the inverse distance weighting method was used to generate a spatial distribution map based on the ground monitoring data (Fig. S5). The surface ozone

remote sensing data (2018) was also used to assess the ozone spatial distribution (Fig. 3).

After comparing these two spatial maps (Fig. S5 and Fig. 3), we found they were very similar: the high-value zone was located in the southeast of Ngari, southeast of Shigatse, south of Lhasa, and northwest of Lhokha, with a mean concentration of ~80 μg/m^3, while the low-value zone was in the east of Nagchu, southwest of Nying, and southeast of Lhokha, with a mean concentration of ~50 μg/m^3. Generally, surface ozone concentrations in Tibet were higher in the southwest and lower in the southeast and northeast. The similarity between ground and remote sensing data suggested that surface ozone remote sensing data (2018) were sufficiently robust.

The spatial correlation of surface ozone in Tibet based on the spatial autocorrelation analysis tool (Moran's *I* index) and the surface ozone remote sensing data (2018) was further calculated. The results (I = 0.06) indicated that there was no significant positive or negative spatial correlation of surface ozone across Tibet (Table S3). The spatial difference of surface ozone in Tibet was broadly consistent with its complex geographical and climatic conditions (Yao et al., 2012).

3.3. Individual effect of influencing factors

Regular linear correlation was conducted between ozone concentrations and meteorological factors from Nagri (west Tibet), Nagchu (north Tibet), and Nying (south Tibet). All data used are from 2015 to 2019 and the linear fitting results (Fig. S6) showed that all relationships are weak with correlation coefficients (R^2) < 0.2. This indicates that the regular linear correlation could not show sound relationship between surface ozone and influencing factors. In addition, positive correlations between RH and ozone concentration were found (Fig. S6), which is obviously contrary to the common understanding (high RH hinders the formation of ozone) (Han et al., 2019; Li et al., 2021; Liu et al., 2011; Wang et al., 2016b). Thus, the linear correlations method is not suitable for sorting out the possible influence factors. Moreover, the relationships obtained in Fig. S6 were based on time-series (from 2015 to 2019) of surface ozone and its related meteorological factors; for better understanding the impacts of individual factors, spatial analysis is needed.

Geodetector method was therefore applied to the spatial remote sensing data (Fig. 3 and Fig. S2) to determine the individual effect of influencing factors. As shown in Fig. 4a, the q values of each influencing factor were ranked as follows: RH (0.58) > NDVI (0.57) > SR (0.51) > DEM (0.46) > WS (0.41) > Temp (0.39) > NO_2 (0.25) > PM_{10} (0.11) > Prep (0.05) > $PM_{2.5}$ (0.03). Meteorological factors (RH, SR, WS, and Temp) and geographic factors (NDVI and DEM) all showed a stronger effect on the surface ozone distribution than anthropogenic factors, such as ozone

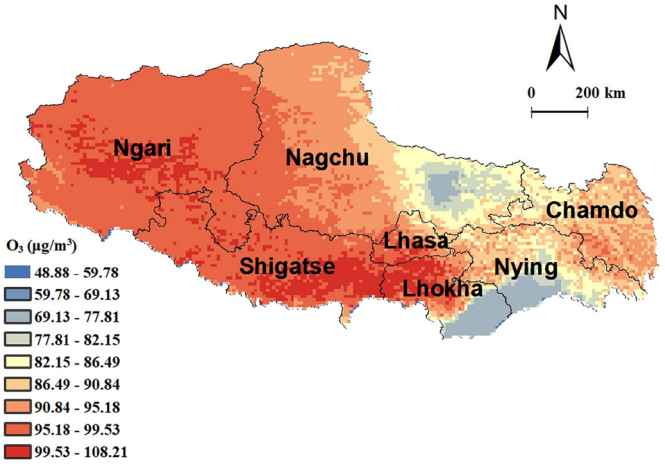

Fig. 3. Spatial distribution of surface ozone across Tibet based on 2018 remote sensing data.

precursor (NO_2), PM_{10}, and $PM_{2.5}$. Similar results have been found in other places: for example, meteorological factors dominated the variation of ozone concentrations in the Western Mediterranean (Sicard et al., 2013), and the geographical conditions of Sierra Nevada directly affected the spatial distribution of surface ozone concentration (Van Ooy and Carroll, 1995).

RH was the dominant influencing factor for surface ozone concentration across Tibet, as it had the greatest q value (0.58) (Fig. 4a). Even on a national scale across China, RH was found as the major influencing factor on surface ozone distribution (Dang et al., 2021; Han et al., 2019; Hu et al., 2021). Similarly, in 74 US cities, RH had the greatest effects on ozone according to a city-specific generalized linear model (Davis et al., 2011). Vegetation cover has a bidirectional influence on ozone pollution, as plants not only release ozone precursors (isoprene) but also absorb ozone through their stomata (Gong et al., 2020). Based on the high q value of NDVI (Fig. 4a), vegetation coverage was the second dominant factor for the Tibetan surface ozone distribution. Additionally, SR and DEM also significantly affected surface ozone distribution (q = ~0.5) (Fig. 4a). Overall, variations in surface ozone concentrations across Tibet were mainly caused by natural factors.

These results are different from some observations in urban areas. For example, in the Beijing–Tianjin–Hebei urban agglomeration, PM_{10} (q = 0.509) and NO_2 (q = 0.43) were the two main influencing factors that affect surface ozone pollution, rather than meteorological factors (Wang et al., 2020b). This is due to the high concentration of ozone precursors in urban regions, promoting the photochemical formation of surface ozone. The comparison indicates that anthropogenic factors and natural reasons control the spatial distribution of surface ozone in urban and remote areas, respectively (Ma et al., 2021).

3.4. Non-linear effect of influencing factors

The non-linear effects of influencing factors on surface ozone across Tibet were also evaluated and are shown in Fig. 4b. According to the results, RH had an inhibitory effect (a decreasing trend in Fig. 4b) on surface ozone concentration, which is contrary to the result of normal linear correlations (Fig. S6) but is consistent with a previous finding that a high surface ozone concentration usually occurs in arid areas (Kim et al., 2021). Similar to RH, the curve for NDVI is also a downward trend (Fig. 4b), which suggests vegetation coverage of Tibet showed a negative relationship with its surface ozone concentration (the higher the vegetation coverage, the lower the surface ozone will be). This indicates that the absorption of surface ozone by vegetation should be the major process, instead of precursor (isoprene) emission in Tibet (Gong et al., 2020).

Contrary to RH and NDVI, the effect trends of DEM, SR, and WS are upward (Fig. 4b), indicating a positive relationship with surface ozone. The high elevation could increase SR intensity, and strong SR drives active photochemical reactions, leading to the increase of surface ozone concentrations (Wang et al., 2017). Strong winds are usually associated with stratospheric ozone invasions which also causes the increase of surface ozone (Wang et al., 2020a). From Fig. 4b, the overall effects of $PM_{2.5}$, PM_{10}, and Prep on the surface ozone across Tibet were stable, which may be related to their small fluctuation range.

3.5. Interaction effects of influencing factors

Since the surface ozone distribution is affected by many factors, the explanatory power of a single factor is usually limited. It is necessary to further explore the interaction effects of different factors. Given the advantages of the interaction detector in the Geodetector, the associated strengths of two different influencing factors on surface ozone distribution across Tibet are calculated and shown in Fig. 5. The significance of the interaction effects between two different factors tested by the ecological detector of Geodetector are listed in Table S4. Generally, the interaction effects of two different factors all showed a nonlinear enhancement compared with those of an individual factor [q(X1∩X2) > q(X1) + q(X2),

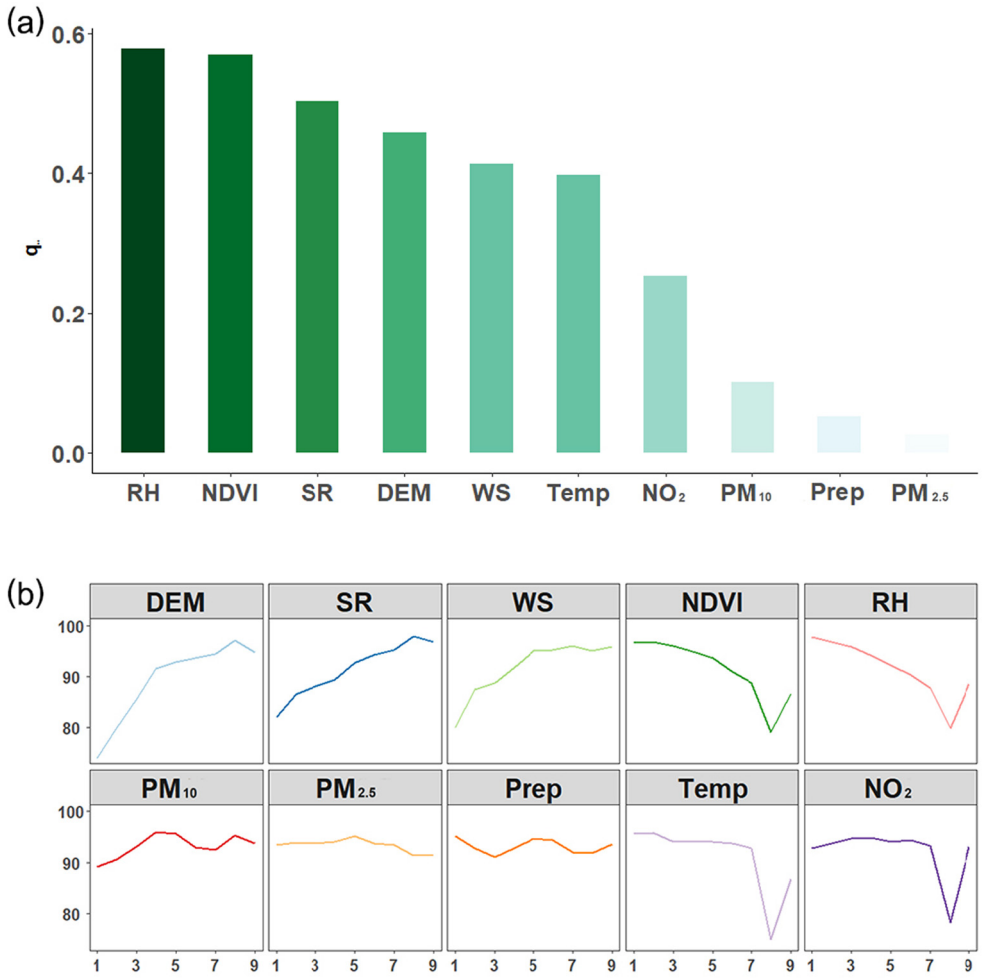

Fig. 4. The q value of the individual factors (a) and the nonlinear effects of each influencing factor (b) on the spatial distribution of surface ozone across Tibet.

where ∩ denotes the interaction between X1 and X2], indicating the interaction effect would further enhance the explanatory power of influencing factors on surface ozone distribution across Tibet.

Among all the interactions, the strength of RH∩PM_{10} reached the highest value (q = 0.77), followed by RH∩$PM_{2.5}$ (q = 0.74) (Fig. 5). This indicates that the combined influence of meteorological factors (such as RH) and pollutant factors (such as PM) exhibit a high impact on surface ozone distribution across Tibet. With both low RH and low concentrations of PM_{10} and $PM_{2.5}$, the SR intensity would be stronger, which promotes ozone formation. Similarly, Tu et al. (2007) also found that lower humidity and less suspended particulate matter were more conducive to surface ozone formation.

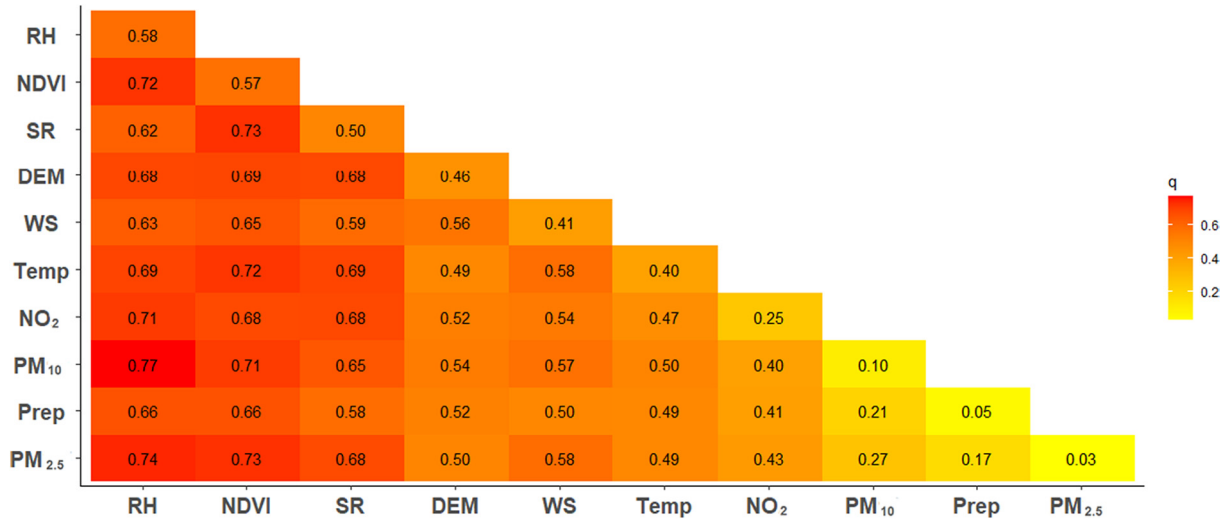

Fig. 5. The q value of the interaction effects for two different influencing factors on surface ozone distribution across Tibet.

The interactions between NDVI and meteorological factors or precursors also dramatically enhanced the influencing strength. The q values of NDVI∩Temp and NDVI∩SR reached 0.72 and 0.73, respectively, while those of NDVI∩$PM_{2.5}$ and NDVI∩PM_{10} were 0.73 and 0.71, respectively (Fig. 5). The enhanced q values of NDVI∩Temp demonstrated that great ozone levels should occur at cold-desert places. Similarly, the strength of the association of NDVI∩SR suggested that high mountain areas, usually sparsely vegetated with greater levels of SR, will have high ozone concentrations.

Although the individual influences of $PM_{2.5}$ and PM_{10} were relatively minor, after associating with NDVI (NDVI∩$PM_{2.5}$, NDVI∩PM_{10}), their joint influences greatly increased (Fig. 5). This also implied that some areas with desertification (low NDVI) and clear sky (low burden of PMs) should contain great ozone concentrations in the near-surface atmosphere.

Concerning NO_2, the interaction effects of RH∩NO_2, NDVI∩NO_2, and SR∩NO_2 were much greater (q = ~0.70) (Fig. 5) than the individual effect (q = 0.25) (Fig. 4a). This indicated that ozone precursors can affect surface ozone distribution, especially under suitable meteorological conditions, such as dry conditions with intense radiation (Shen et al., 2014). However, compared with RH, NDVI, and SR, the associated impacts of other factors (DEM, WS, Temp, Prep) were relatively weak (Fig. 5).

3.6. Explanation for the Tibetan ozone spatiotemporal distribution feature

The above spatial distribution map of surface ozone across Tibet shows that the high-value surface ozone is located in Ngari, south of Shigatse, and west of Lhokha, and Lhasa, while the low-value zone is scattered in Nagchu and Nying (Fig. 3). The Geodetector results can explain why some places displayed high-value concentrations, whereas others were low-value.

The Geodetector results indicated that cold-desert places (NDVI∩Temp and NDVI∩SR) should exhibit high ozone levels. Ngari is characterized by its cold (average Temp ~0 °C), desert landscape (low NDVI), and strong SR (~5300 Wh/m^2/day) (Wang et al., 2016a), which explains the high ozone concentration in this region.

South Shigatse and west Lhokha contain a series of great mountains, including the edge of the Himalayas (Fig. 1). As the main landscape of these regions is glacier-covered mountain (Wang et al., 2012), SR is remarkably high and the NDVI values are generally low. Due to the strong impact of NDVI∩SR, the ozone levels in these regions are relatively high (>100 μg/m^3, Fig. 3).

As Lhasa is the capital city of Tibet, local emissions of NO_2 and other ozone precursors are possible there, such as vehicle exhaust gas (Yin et al., 2019). Local emissions of NO_2, coupled with the strong SR (Lhasa is also called the city of sunshine), will promote the formation of ozone (q of NO_2∩SR = 0.68, Fig. 5), and therefore ozone levels in Lhasa are relatively high (Fig. 3).

Surface ozone concentrations in Nying were low (Fig. 3), which is the result of high RH and high NDVI (q of RH∩NDVI = 0.72, Fig. 5). Nying contains a large area of forest, which will absorb atmospheric ozone; it is also at the entry point of the Indian monsoon, so the great Prep (>600 mm) and high RH in the air (Gao et al., 2021) decrease the concentrations of ozone precursors and slow down the speed of photochemical reactions. Thus, ozone concentrations in Nying are relatively low (<70 μg/m^3) (Fig. 3).

Ozone concentrations in the east Nagchu region are also lower, as sandstorms occasionally occur there (Chen et al., 2019). During sandstorm periods, there is a high burden of particulate matter. When levels of PM_{10} (dominant size for sandstorm) exceeded 550 μg/m^3, the surface ozone concentrations were all below 52 μg/m^3, which is much lower than the average values (Fig. S7). PMs can shield SR and then result in low ozone concentration (Wang et al., 2020a).

Apart from the phenomena in Tibet, other evidence can also be found in remote regions of the world. For example: in the Front Range Mountains of Colorado, surface ozone was observed to increase with altitude, confirming that association of high SR and low NDVI would aggravate ozone (Brodin et al., 2010). In the central part of Russia, the emission of atmospheric pollution (NO_2) and strong SR was related to ozone accumulation (Stepanov et al., 2019), similar to the findings in Lhasa (Yin et al., 2019). Observations in Gozo island showed that changes in RH and vegetation affect the surface ozone variation (Saliba et al., 2008). The impact of particulates on ozone precursors, which shows a negative correlation between PM_{10} and surface ozone, has also been observed in Kannur, India (Nishanth et al., 2014).

Overall, based on results from our study the other worldwide studies, the associated impacts of low RH, strong SR and poor vegetation coverage are likely the reasons for elevated surface ozone in atmosphere of remote regions.

4. Conclusions

This study confirms that the formation and distribution of surface ozone across Tibet are mainly controlled by natural factors rather than anthropogenic activities. It has been found in Tibet and similar areas with sparse vegetation and dry climates can have high surface ozone concentrations; high-altitude areas that receive more SR usually contain great ozone level. The elevated temperature and low relative humidity caused by global warming may contribute to the continuous increase of surface ozone in remote areas. To further understand how surface ozone forms in remote alpine regions, more long-term ground monitoring of ozone should be conducted in future. Additionally, the stratosphere-to-troposphere transport of ozone must also be considered to quantify the effects of the downward transport of ozone.

Author contributions statement

Yan Chen: Conceptualization, Methodology, Investigation, Data curation, Writing - Original Draft. **Yunqiao Zhou:** Formal analysis, Writing - review & editing, Visualization. **NixiaCiren:** Writing - review & editing. **Huifang Zhang:** Writing - review & editing. **Caihong Wang:** Writing - review & editing. **GesangDeji:** Writing - review & editing. **Xiaoping Wang:** Conceptualization, Writing - review & editing, Supervision, Project administration, Funding acquisition

Declaration of Competing Interest

The authors declare that they have no known competing financial interests or personal relationships that could have appeared to influence the work reported in this paper.

Acknowledgments

This study was supported by the Strategic Priority Research Program of the Chinese Academy of Sciences, the Pan-Third Pole Environment Study for a Green Silk Road (Pan-TPE) (XDA2004050202), the National Natural Science Foundation of China (41925032, 42107438), and the China Postdoctoral Science Foundation (2020M680696). We thank Dr. Jing Wei from the University of Maryland for providing us with the ChinaHighO_3 data from the CHAP dataset (available at https://weijing-rs.github.io/product.html).

Appendix A. Supplementary data

Supplementary data to this article can be found online at https://doi.org/10.1016/j.scitotenv.2021.152651.

References

Agathokleous, E., Feng, Z., Oksanen, E., Sicard, P., Wang, Q., Saitanis, C.J., Araminiene, V., Blande, J.D., Hayes, F., Calatayud, V., Domingos, M., Veresoglou, S.D., Peñuelas, J., Wardle, D.A., Marco, A.D., Li, Z., Harmens, H., Yuan, X., Vitale, M., Paoletti, E., 2020. Ozone affects plant, insect, and soil microbial communities: a threat to terrestrial ecosystems and biodiversity. Sci. Adv. 6, eabc1176.

Avnery, S., Mauzerall, D.L., Liu, J., Horowitz, L.W., 2011. Global crop yield reductions due to surface ozone exposure: 1. Year 2000 crop production losses and economic damage. Atmos. Environ. 45, 2284–2296.
Brodin, M., Helmig, D., Oltmans, S., 2010. Seasonal ozone behavior along an elevation gradient in the Colorado Front Range Mountains. Atmos. Environ. 44, 5305–5315.
Burley, J.D., Bytnerowicz, A., 2011. Surface ozone in the White Mountains of California. Atmos. Environ. 45, 4591–4602.
Chen, K., Zhou, L., Chen, X., Bi, J., Kinney, P.L., 2017. Acute effect of ozone exposure on daily mortality in seven cities of Jiangsu Province, China: no clear evidence for threshold. Environ. Res. 155, 235–241.
Chen, P.F., Kang, S.C., Yang, J.H., Pu, T., Li, C.L., Guo, J.M., Tripathee, L., 2019. Spatial and temporal variations of gaseous and particulate pollutants in six sites in Tibet, China, during 2016–2017. Aerosol Air Qual. Res. 19, 516–527.
Chen, X., Zhong, B.Q., Huang, F.X., Wang, X.M., Sarkar, S., Jia, S.G., Deng, X.J., Chen, D.H., Shao, M., 2020. The role of natural factors in constraining long-term tropospheric ozone trends over southern China. Atmos. Environ. 220, 117060.
Cooper, O.R., Langford, A.O., Parrish, D.D., Fahey, D.W., 2015. Challenges of a lowered U.S. ozone standard. Science 348, 1096–1097.
Cristofanelli, P., Bracci, A., Sprenger, M., Marinoni, A., Bonafè, U., Calzolari, F., Duchi, R., Laj, P., Pichon, J.M., Roccato, F., Venzac, H., Vuillermoz, E., Bonasoni, P., 2010. Tropospheric ozone variations at the Nepal climate observatory-pyramid (Himalayas, 5079 m a.s.l.) and influence of deep stratospheric intrusion events. Atmos. Chem. Phys. 10, 6537–6549.
Dang, R.J., Liao, H., Fu, Y., 2021. Quantifying the anthropogenic and meteorological influences on summertime surface ozone in China over 2012–2017. Sci. Total Environ. 754, 142394.
Davis, J., Cox, W., Reff, A., Dolwick, P., 2011. A comparison of CMAQ-based and observation-based statistical models relating ozone to meteorological parameters. Atmos. Environ. 45, 3481–3487.
Derwent, R.G., Manning, A.J., Simmonds, P.G., Spain, T.G., O'Doherty, S., 2018. Long-term trends in ozone in baseline and european regionally-polluted air at Mace head, Ireland over a 30-year period. Atmos. Environ. 179, 279–287.
Feng, Z., Hu, E., Wang, X., Jiang, L., Liu, X., 2015. Ground-level O_3 pollution and its impacts on food crops in China: a review. Environ. Pollut. 199, 42–48.
Gao, J.J., Ma, P.F., Du, J., Huang, X.Q., 2021. Spatial distribution of extreme precipitation in the tibetan plateau and effects of external forcing factors based on generalized pareto distribution. Water Supply 21, 1253–1262.
Gong, C., Lei, Y.D., Ma, Y.M., Yue, X., Liao, H., 2020. Ozone–vegetation feedback through dry deposition and isoprene emissions in a global chemistry–carbon–climate model. Atmos. Chem. Phys. 20, 3841–3857.
Han, Y.M., Gong, Z.H., Ye, J.H., Liu, P.F., McKinney, K.A., Martin, S.T., 2019. Quantifying the role of the relative humidity-dependent physical state of organic particulate matter in the uptake of semivolatile organic molecules. Environ. Sci. Technol. 53, 13209–13218.
Helmig, D., Oltmans, S.J., Carlson, D., Lamarque, J.-F., Jones, A., Labuschagne, C., Anlauf, K., Hayden, K., 2007. A review of surface ozone in the polar regions. Atmos. Environ. 41, 5138–5161.
Hu, C.Y., Kang, P., Jaffe, D.A., Li, C.K., Zhang, X.L., Wu, K., Zhou, M.W., 2021. Understanding the impact of meteorology on ozone in 334 cities of China. Atmos. Environ. 248, 118221.
Kim, H.C., Lee, D., Ngan, F., Kim, B.-U., Kim, S., Bae, C., Yoon, J.H., 2021. Synoptic weather and surface ozone concentration in South Korea. Atmos. Environ. 244, 117985.
Li, M.Y., Yu, S.C., Chen, X., Li, Z., Zhang, Y.B., Wang, L.Q., Liu, W.P., Li, P.F., Lichtfouse, E., Rosenfeld, D., Seinfeld, J.H., 2021. Large scale control of surface ozone by relative humidity observed during warm seasons in China. Environ. Chem. Lett. 19, 3981–3989.
Lin, W., Xu, X., Zheng, X., Dawa, J., Baima, C., Ma, J., 2015. Two-year measurements of surface ozone at Dangxiong, a remote highland site in the Tibetan Plateau. J. Environ. Sci. 31, 133–145.
Liu, P.F., Zhao, C.S., Göbel, T., Hallbauer, E., Nowak, A., Ran, L., Xu, W.Y., Deng, Z.Z., Ma, N., Midenberger, K., Henning, S., Stratmann, F., Wiedensohler, A., 2011. Hygroscopic properties of aerosol particles at high relative humidity and their diurnal variations in the North China plain. Atmos. Chem. Phys. 11, 3479–3494.
Liu, H., Liu, S., Xue, B., Lv, Z., Meng, Z., Yang, X., Xue, T., Yu, Q., He, K., 2018. Ground-level ozone pollution and its health impacts in China. Atmos. Environ. 173, 223–230.
Ma, J., Lin, W.L., Zheng, X.D., Xu, X.B., Li, Z., Yang, L.L., 2014. Influence of air mass downward transport on the variability of surface ozone at Xianggelila Regional Atmosphere Background Station, Southwest China. Atmos. Chem. Phys. 14, 5311–5325.
Ma, M., Yao, G., Guo, J., Bai, K., 2021. Distinct spatiotemporal variation patterns of surface ozone in China due to diverse influential factors. J. Environ. Manag. 288, 112368.
Maji, K.J., Namdeo, A., 2021. Continuous increases of surface ozone and associated premature mortality growth in China during 2015–2019. Environ. Pollut. 269, 116183.
Neu, J.L., Flury, T., Manney, G.L., Santee, M.L., Livesey, N.J., Worden, J., 2014. Tropospheric ozone variations governed by changes in stratospheric circulation. Nature Geosci. 7, 340–344.
Nishanth, T., Praseed, K.M., Kumar, M.K.S., Valsaraj, K.T., 2014. Influence of ozone precursors and PM_{10} on the variation of surface O_3 over Kannur, India. Atmos. Res. 138, 112–124.
Pierre, S., 2021. Ground-level ozone over time: an observation-based global overview. Curr. Opin. Environ. Sci. Health 19, 100226.
Ran, L., Lin, W.L., Deji, Y.Z., La, B., Tsering, P.M., Xu, X.B., Wang, W., 2014. Surface gas pollutants in Lhasa, a highland city of Tibet – current levels and pollution implications. Atmos. Chem. Phys. 14, 10721–10730.
Saliba, M., Ellul, R., Camilleri, L., Güsten, H., 2008. A 10-year study of background surface ozone concentrations on the island of Gozo in the Central Mediterranean. J. Atmos. Chem. 60, 117–135.
Shen, Z., Cao, J., Zhang, L., Zhao, Z., Dong, J., Wang, L., Wang, Q., Li, G., Liu, S., Zhang, Q., 2014. Characteristics of surface O_3 over Qinghai Lake area in Northeast Tibetan Plateau, China. Sci. Total. Environ. 500–501, 295–301.
Shu, L., Wang, T.J., Han, H., Xie, M., Chen, P.L., Li, M.M., Wu, H., 2020. Summertime ozone pollution in the Yangtze River Delta of eastern China during 2013–2017: synoptic impacts and source apportionment. Environ. Pollut. 257, 113631.
Sicard, P., De Marco, A., Troussier, F., Renou, C., Vas, N., Paoletti, E., 2013. Decrease in surface ozone concentrations at Mediterranean remote sites and increase in the cities. Atmos. Environ. 79, 705–715.
Stepanov, E., Kotelnikov, S., Ratushnyk, G., Bogun, I., 2019. Peak concentrations of ground-level ozone during the summer heat waves of 2010 and 2016 in the background region of the Kirov region of the Russian Federation. IOP Conf. Ser.: Earth Environ. Sci. 390, 012035.
Sunwoo, Y., Carmichael, G.R., 1994. Characteristics of background surface ozone in Japan. Atoms. Environ. 28, 25–37.
Tarasova, O.A., Senik, I.A., Sosonkin, M.G., Cui, J., Staehelin, J., Prévôt, A.S.H., 2009. Surface ozone at the caucasian site Kislovodsk High Mountain station and the Swiss Alpine site Jungfraujoch: data analysis and trends (1990–2006). Atmos. Chem. Phys. 9, 4157–4175.
Tu, J., Xia, Z.-G., Wang, H., Li, W., 2007. Temporal variations in surface ozone and its precursors and meteorological effects at an urban site in China. Atmos. Res. 85, 310–337.
Turner, M.C., Jerrett, M., Pope, C.A., Krewski, D., Gapstur, S.M., Diver, W.R., Beckerman, B.S., Marshall, J.D., Su, J., Crouse, D.L., Burnett, R.T., 2016. Long-term ozone exposure and mortality in a large prospective study. Am. J. Respir. Crit. Care Med. 193, 1134–1142.
Van Ooy, D.J., Carroll, J.J., 1995. The spatial variation of ozone climatology on the Western slope of the Sierra Nevada. Atmos. Environ. 29, 1319–1330.
Wang, J., Xu, C., 2017. Geodetector: principle and prospective. Acta Geograph. Sin. 72, 116–134 (in Chinese).
Wang, J.F., Li, X.H., Christakos, G., Liao, Y.L., Zhang, T., Gu, X., Zheng, X.Y., 2010. Geographical detectors-based health risk assessment and its application in the neural tube defects study of the Heshun Region, China. Int. J. Geogr. Inf. Sci. 24, 107–127.
Wang, X., Liu, S.Y., Guo, W.Q., Yao, X.J., Jiang, Z.L., Han, Y.S., 2012. Using remote sensing data to quantify changes in glacial lakes in the Chinese Himalaya. Mt. Res. Dev. 32, 203–212.
Wang, S., Zhang, L.F., Fu, D.J., Lu, X., Xu, T.X., Tong, Q.X., 2016a. Selecting photovoltaic generation sites in Tibet using remote sensing and geographic analysis. Sol. Energy 133, 85–93.
Wang, Y.J., Luo, H., Jia, L., Ge, S.S., 2016b. Effect of particle water on ozone and secondary organic aerosol formation from benzene–NO_2–NaCl irradiations. Atmos. Environ. 140, 386–394.
Wang, W., Cheng, T., Gu, X., Chen, H., Guo, H., Wang, Y., Bao, F., Shi, S., Xu, B., Zuo, X., Meng, C., Zhang, X., 2017. Assessing spatial and temporal patterns of observed ground-level ozone in China. Sci. Rep. 7, 3651.
Wang, Y., Gao, W., Wang, S., Song, T., Gong, Z., Ji, D., Wang, L., Liu, Z., Tang, G., Huo, Y., Tian, S., Li, J., Li, M., Yang, Y., Chu, B., Petäjä, T., Kerminen, V.-M., He, H., Hao, J., Kulmala, M., Wang, Y., Zhang, Y., 2020a. Contrasting trends of $PM_{2.5}$ and surface-ozone concentrations in China from 2013 to 2017. Natl. Sci. Rev. 7, 1331–1339.
Wang, Z., Li, J., Liang, L., 2020b. Spatio-temporal evolution of ozone pollution and its influencing factors in the Beijing-Tianjin-Hebei Urban Agglomeration. Environ. Pollut. 256, 113419.
Wei, J., Li, Z., Li, K., Dickerson, R., Pinker, R., Wang, J., Liu, X., Sun, L., Xue, W., Cribb, M., 2022. Full-coverage mapping and spatiotemporal variations of ground-level ozone (O_3) pollution from 2013 to 2020 across China. Remote Sens. Environ, 112775 https://doi.org/10.1016/j.rse.2021.11277 In press.
Xu, W., Lin, W., Xu, X., Tang, J., Huang, J., Wu, H., Zhang, X., 2016. Long-term trends of surface ozone and its influencing factors at the Mt Waliguan GAW station, China - Part 1: Overall trends and characteristics. Atmos. Chem. Phys. 16, 6191–6205.
Xu, J.W., Huang, X., Wang, N., Li, Y.Y., Ding, A.J., 2021. Understanding ozone pollution in the Yangtze River Delta of eastern China from the perspective of diurnal cycles. Sci. Total Environ. 752, 141928.
Xue, L., Wang, T., Zhang, J., Zhang, X., Deliger, C., Ding, A., Zhou, X., Wu, W., Tang, J., Zhang, Q., Wang, W., 2011. Source of surface ozone and reactive nitrogen speciation at Mount Waliguan in western China: new insights from the 2006 summer study. J. Geophys. Res - Atmos. 116, D07306.
Yao, T., Thompson, L.G., Mosbrugger, V., Zhang, F., Ma, Y., Luo, T., Xu, B., Yang, X., Joswiak, D.R., Wang, W., Joswiak, M.E., Devkota, L.P., Tayal, S., Jilani, R., Fayziev, R., 2012. Third pole environment (TPE). Environ. Dev. 3, 52–64.
Yeo, M.J., Kim, Y.P., 2021. Long-term trends of surface ozone in Korea. J. Clean. Prod. 294, 125352.
Yin, X., Kang, S., de Foy, B., Cong, Z., Luo, J., Zhang, L., Ma, Y., Zhang, G., Rupakheti, D., Zhang, Q., 2017. Surface ozone at Nam Co in the inland Tibetan Plateau: variation, synthesis comparison and regional representativeness. Atmos. Chem. Phys. 17, 11293–11311.
Yin, X., Foy, B., Wu, K., Feng, C., Kang, S., Zhang, Q., 2019. Gaseous and particulate pollutants in Lhasa, Tibet during 2013–2017: spatial variability, temporal variations and implications. Environ. Pollut. 253, 68–77.
Zhan, Y., Luo, Y.Z., Deng, X.F., Grieneisen, M.L., Zhang, M.H., Di, B.F., 2018. Spatiotemporal prediction of daily ambient ozone levels across China using random forest for human exposure assessment. Environ. Pollut. 233, 464–473.
Zhang, L., Jin, L.J., Zhao, T.L., Yin, Y., Zhu, B., Shan, Y.P., Guo, X.M., Tan, C.H., Gao, J.H., Wang, H.L., 2015. Diurnal variation of surface ozone in mountainous areas: case study of Mt. Huang, East China. Sci. Total Environ. 538, 583–590.